International Journal of Recent Technology and Engineering (IJRTE)
ISSN: 2277-3878 (Online), Volume-9 Issue-1, May 2020

CFD Simulation of Flow Characteristics on Semi-Submersible Platforms

T Sai Shyam, P R Jishnu, R Harish

Abstract: ***In this paper we present the turbulent flow around a semi-submersible platform, modelled using Ansys Fluent. The computational domain is designed as a rectangular horizontal channel with the semi-submersible platform mounted inside the channel. The top, bottom, left and right walls of the channel are treated with no slip boundary condition. The front and back walls are specified with velocity inlet and pressure outlet boundary conditions. The semi-submersible platform is designed with of two pontoons, four square columns and two bracings. The problem is modelled as three dimensional, transient, incompressible flow and turbulence is modelled using Large eddy simulation (LES) turbulence model. The computational domain is meshed to 4,72,749 hexahedral mesh cells. Parametric study is performed by varying the Reynolds number (Re) in the range of*** $10^4 \leq Re \leq 10^6$ ***and also the shape of the columns. The investigation is carried out by plotting stream function, velocity and pressure contours. We observe vortex shedding and flow separation between the front and back columns of the semi-submersible platform. As we increase the Reynolds number the intensity of flow separation also increases. The transient flow characteristics of the lift and drag forces are evaluated by plotting the coefficients of lift and drag for different Reynolds number and column shapes.***

Keywords**: *CFD, LES turbulence model, Reynolds number, Semi-submersible platform.***

I. INTRODUCTION

Semi-submersible platforms are one of the most widely used offshore structures for oil and gas exploration in the sea. The semi-submersibles are often working under various complex conditions inside the sea hence the overall analysis of the flow characteristics of a semi-submersible is mandatory. In this paper, we are attempting to reveal the flow characteristics of a four-column semi-submersible platform using ANSYS Fluent by considering the turbulent flow around the platform. The method of parametric study is performed by varying the Reynolds number (Re) in the range of $10^4 \leq Re \leq 10^6$ and the shape of the columns. The drag and lift forces playing a relevant role in the functioning of the semi-submersible. So in this paper, we are also investigating the lift and drag of the semi-submersible. Liu et al. [1] performed an excellent study to find out the flow characteristics over a four square shaped cylinders in a square arrangement. They have considered spacing ratios and array attack angles for parametric study and have found out both the drag and lift forces experienced around the cylindrical columns are showing a very small difference for different L/D values, and the fluctuating forces touches its maximum when the L/D value equals to 4.14. The paper also shows that lift force reaches its peak for downstream cylinders at an angle of $\alpha = 15°$. Goncalves et al. [2] carried out an investigation on Vortex Induced Motion (VIM) of a four square column semi-submersible. They conducted some model tests to analyse the impact of hull appendages and various headings. The final results consist of details about various motions including the in-line motion, transverse motion and yaw motions, along with this combined motions in the XY plane and analysis of both drag and lift forces. They concluded that vortex induced motion in transverse direction appears only in a range of a reduced velocity from 4.0 to 14.0. The largest transverse amplitude occurs around 40% width of the column about the incidences angles of 30^o and 45^o. They also verified the occurrence of largest yaw motion was for 0^o incidence and at 4.5^o incidence the maximum amplitudes have appeared. Ma et al. [3] inspect the structural dynamic responses over a short term sea conditions under the presence of both wind and load. They eventually obtained a relation between wind and waves. From this they disclosed a correlation between the speed of wind and wave height enhanced by using Mixture Simulation method, then they expanded Wave Scatter Diagram and time series of wind/wave pressure over the platform converted by Workbench-AQWA. Holland et al. [4] performed a full scale CFD analysis to study the transverse forces created by the vortex shedding with the current velocities in the Gulf of Mexico. They validate that the helical strakes which are embedded to the geometry helps to terminate the coherence of the vortex shedding and numerically investigated the performance of these strakes. Xiao et al. [5] conducted a three-dimensional numerical simulations and detailed study to investigate the pontoon effect on the Vortex Induced Motion (VIM) of a four-column arrangement without pontoons and two semi-submersible platforms.

Manuscript received on April 02, 2020.
Revised Manuscript received on April 15, 2020.
Manuscript published on May 30, 2020.
* Correspondence Author
T Sai Shyam, School of Mechanical Engineering, Vellore Institute of Technology Chennai, Tamilnadu-600127, India. Email: saishyam.t2016@vitstudent.ac.in
P R Jishnu, School of Mechanical Engineering, Vellore Institute of Technology Chennnai, **Tamilnadu**-600127, India. Email: jishnup.r2016@vitstudent.ac.in
R Harish*, Assistant Professor, School of Mechanical Engineering, Vellore Institute of Technology Chennai, Tamilnadu-600127, India. Email: harish.r@vit.ac.in

The paper summarizes that the most significant transverse responses was shows by the four column arrangement without pontoons and yaw motions at 0◦ angle and 45◦ angle of incidences showing to the maxima of fluctuating lift forces produced by the well-established wake. Wei et al.

[6] suggest a mathematical model which deals with the bracings on buoyancy, pitch motion on buoyancy, and the nonlinear effects of heave motion on pitch restoring coefficient. They executed numerical simulations and some regular wave tests to examine the coupled motion characteristics and to verify the proposed mathematical model. They observed a unique pitch-motion profile and a double-period phenomenon and good agreements between nonlinear numerical and experimental results to verify the potential of the suggested mathematical model to predict motion instability and precisely simulate the nonlinear effects. By using the proposed verified model, the factors influencing the motion instability were studied and measures to reduce instability were recommended. Tian et al. [7] investigated the motion coupling on the resonance characteristics of a semi-submersible platform and the nonlinear effects of bracings and an improved mathematical model based on potential theory is proposed under irregular wave conditions to simulate the motion response of a semi-submersible platform and results the nonlinear hydrostatic effect of bracings cause the increase of resonance frequency as the motion amplitude increases, whereas the coupling and the hydrodynamic force on the bracings only affect the resonance spectral peak amplitude.

Sharma et al. [8] has evaluated and has given an account on the confrontation facing semi-submersible design, the design of perfect alternative for a selected operating depth and also provided all designing measurements. Odijie et al. [9] reviewed recent contributions in the industrial and academic areas to the development of column stabilized semi-submersible hulls that are used for deep water operations and it also provides a summary of the motion and structural attachments of semi-submersibles. Ghafari et al. [10] examined the dynamic responses features of the floating platforms in the second-order stokes incident wave in ANSYS/AQWA software using the boundary element method for both frequency domain and time domain and the results accurately show that as the platforms come closer to each other, the values of diffraction force, motions and the oscillation of mooring line tension for the semi-submersible platform decrease. Additionally, they revealed that as the wave length increases, it also results in increase of the motions of semi-submersible platform.

II. MATHEMATICAL MODELLING AND NUMERICAL METHOD

The computational domain considered in the present study is of 15 m long, 10 m wide and 10 m high. The semisubmersible is 1.32 m long, 0.81 m wide and 0.48 m high and is centrally located at a distance of 5 m from the inlet wall. The front and back faces of the domain are considered as the inlet and outlet while the top, bottom, left and right faces are specified as stationary walls. The numerical simulations are performed by using Ansys Fluent, where the problem is modelled using turbulent flow of water. The turbulent flow problem is modelled for the velocity fields by solving the Reynolds Averaged Navier-Stokes (RANS) equation. The turbulence is modelled by Large eddy simulation (LES) turbulence model for the kinetic energy and dissipation rate. The time averaged governing equations are as follows:

$$\frac{\partial \overline{u_i}}{\partial t} + \frac{\partial \overline{u_i}}{\partial x_i} = 0 \tag{1}$$

$$\frac{\partial \overline{u_i}}{\partial t} + \overline{u_j}\frac{\partial \overline{u_i}}{\partial x_j} = -\frac{1}{\rho}\frac{\partial \overline{p}}{\partial \overline{x_i}} + \frac{\partial}{\partial x_j}\left[\upsilon \frac{\partial \overline{u_i}}{\partial x_j} - \overline{u_i' u_j'}\right] \tag{2}$$

$$\frac{\partial k}{\partial t} + \overline{u_i}\frac{\partial k}{\partial x_i} = \frac{\partial}{\partial x_i}\left[\frac{\upsilon_t}{\sigma_k}\frac{\partial k}{\partial x_i}\right] + \upsilon_t\left[\frac{\partial \overline{u_i}}{\partial x_j} + \frac{\partial \overline{u_j}}{\partial x_i}\right]\frac{\partial \overline{u_i}}{\partial x_j} - \varepsilon \tag{3}$$

$$\frac{\partial \varepsilon}{\partial t} + \overline{u_i}\frac{\partial \varepsilon}{\partial x_i} = \frac{\partial}{\partial x_i}\left[\frac{\upsilon_t}{\sigma_k}\frac{\partial \varepsilon}{\partial x_i}\right] + C_{1\varepsilon}\frac{\varepsilon}{k}\upsilon_t\left[\frac{\partial \overline{u_i}}{\partial x_j} + \frac{\partial \overline{u_j}}{\partial x_i}\right]\frac{\partial \overline{u_i}}{\partial x_j} - C_{2\varepsilon}\frac{\varepsilon^2}{k} \tag{4}$$

Here, 'u' indicates the velocity fields, 'k' and 'ε' represents the kinetic energy and dissipation fields, and 'ρ' indicates the density of fluid. The lifting force acting on a body in any fluid can be calculated using

$$F_l = ½.C_l.\rho.v^2.A \tag{5}$$

'F_l' represents the lifting force, 'C_l' indicates the lifting coefficient, 'ρ' is the density of fluid, 'v' is the flow velocity and A is the area of the body

$$F_d = ½.C_d.\rho.v^2.A \tag{6}$$

'F_d' represents the drag force, 'C_l' indicates the drag coefficient, 'ρ' is the density of fluid, 'v' is the flow velocity and A is the area of the body.

For simulation, the pressure and velocity are coupled using Coupled algorithm. Spatial discretization for gradient is least squares cell based, pressure is second order and momentum is second order upwind. Second order implicit transient formulation is selected.

III. RESULTS AND DISCUSSION

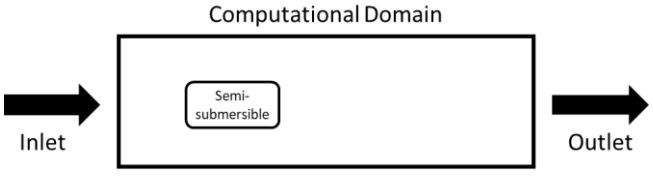

Fig. 1. Schematic diagram of the setup

Fig. 1 represents the fluid flow considered in the present study. We simulate the flow by varying the Reynolds number in the range of $10^4 \leq Re \leq 10^6$ corresponding to the inlet of the computational domain.

Phenomena such as vortex shedding and flow separation are observed near the location of the semi-submersible. The Reynolds number is varied by changing the inlet velocity. In this paper, we consider three different cases.

That is, the characteristics of the flow when the inlet velocity is 0.1 m/s, 5 m/s and 10 m/s. For each of these cases, we graphically represent the velocity streamlines, velocity contours and pressure contours. Along with them, plots of coefficients of lift and drag are also included.

Table – I: Reynolds number values corresponding to inlet velocities

Sl No.	Inlet Velocity (m/s)	Reynolds Number (Re)
1	0.1	5.58×10^4
2	5	2.79×10^6
3	10	5.58×10^6

Table – I show the corresponding Reynolds number values for the three different cases of inlet velocity.

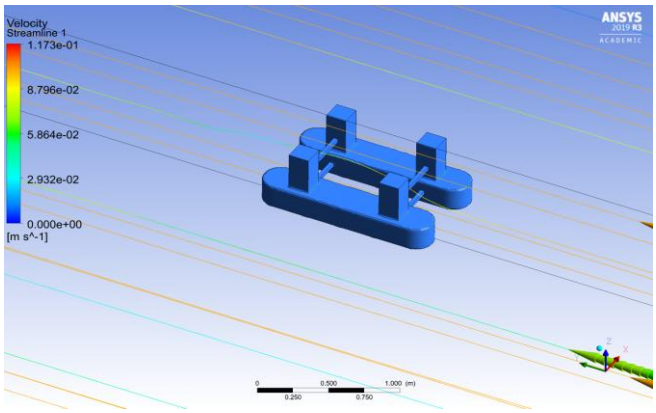

Fig. 2. (a). Velocity streamlines when v = 0.1 m/s

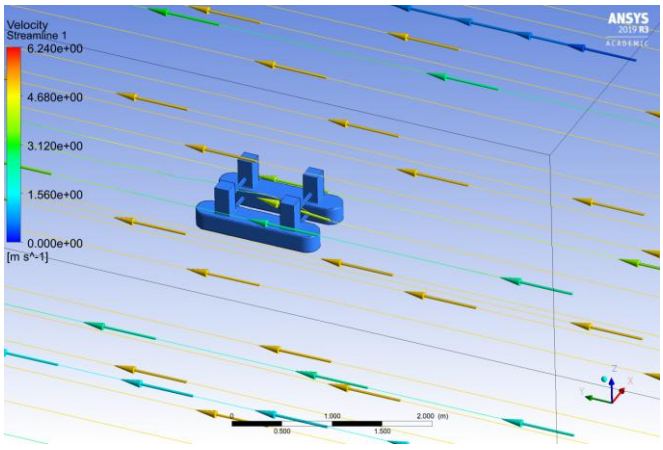

Fig. 2. (b). Velocity streamlines when v = 5 m/s

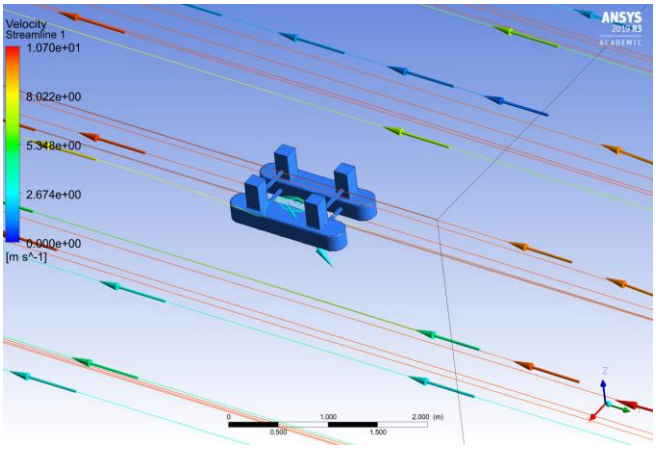

Fig. 2. (c). Velocity Streamlines when v = 10 m/s

Fig. 2. (a), Fig. 2. (b) and Fig. 2. (c) represents the velocity streamlines for the three inlet velocity cases. We can see that as the velocity increases, the flow in and around the semi-submersible is also undergoing changes. The streamlines passing through the centre of the semi-submersible is following an unusual path. It becomes more irregular with the increase in inlet velocity. In Fig. 2. (c), when the inlet velocity is 10 m/s, the streamline in between the pontoons follows a swirling like path which indicates the vortex shedding phenomena. It implies that vortex shedding will take place between the two pontoons of the semi-submersible and it intensifies with increase in velocity.

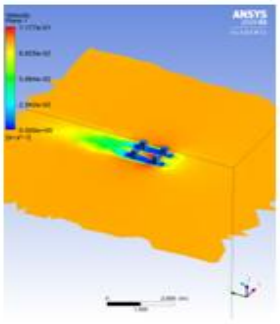

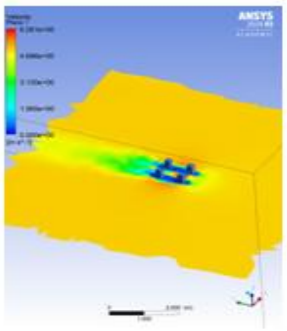

Fig. 3. (a). Velocity contour when v = 0.1 m/s

Fig. 3. (b). Velocity contour when v = 5 m/s

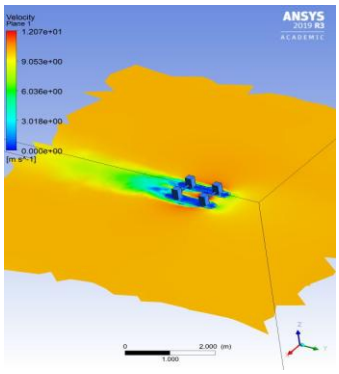

Fig. 3. (c). Velocity contour when v = 10 m/s

Fig. 3. (a), Fig. 3. (b) and Fig. 3. (c) shows the velocity contours along a plane parallel to the pontoons. It can be seen that the velocity is highest at the centre region indicating vortex shedding. Flow separation is illustrated very evidently using different colours. We observe that as the inlet velocity increases, the distance of separation of flow also increases. For the highest velocity case, the flow reunites at a distant location compared to the other two cases.

We see that with the increase in inlet velocity the trend does not change rather being intensified. Same situation is seen in the case of pressure contours. They too follow the same trend. The pressure contours in each case are having same pattern but a higher value than the previous case. Fig. 4. (a), Fig. 4. (b) and Fig. 4. (c) depicts the pressure contours.

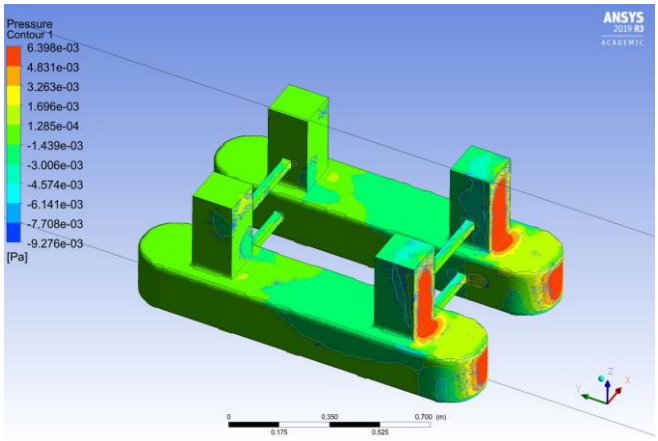

Fig. 4. (a). Pressure contour when v = 0.1 m/s

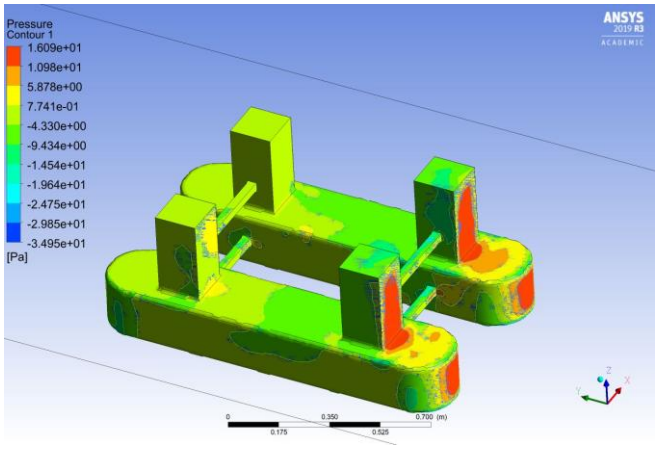

Fig. 4. (b). Pressure contour when v = 5 m/s

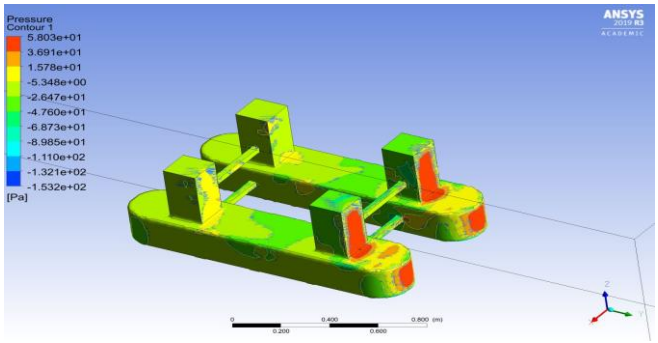

Fig. 4. (c). Pressure contour when v = 10 m/s

The lift and drag experienced by the semi-submersible is very significant. We plotted the lift and drag coefficients (C_l and C_d) against flow-time. Hence we were able to find out the relation between the inlet velocity and the coefficients of lift and drag.

Fig. 5. (a) shows the plot of drag coefficient (C_d) when the inlet velocity is 0.1 m/s against the flow-time. The maximum value C_d attains in this span is 0.010 and the minimum is -0.005. In Fig. 5. (b), the maximum C_d value is 0.0020 and minimum is -0.0015. This is when the inlet velocity is 5 m/s. But we can see huge number of fluctuations compared to the previous case. Same trend can be seen when the velocity is 10 m/s which is depicted in Fig. 5. (c). There are lot of fluctuations. The maximum value of C_d is 0.0025 and minimum is -0.0025.

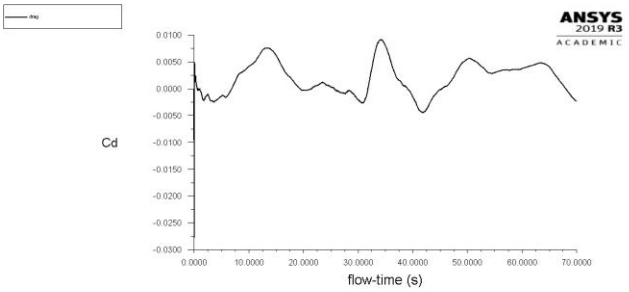

Fig. 5. (a). Coefficient of drag vs flow-time when v = 0.1 m/s

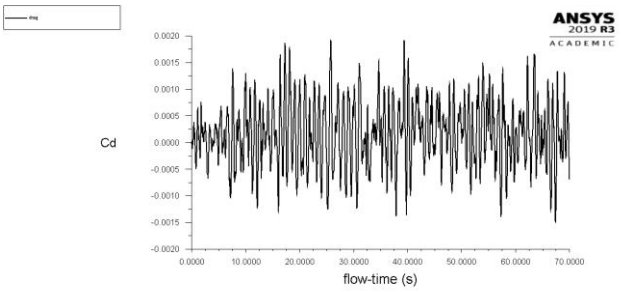

Fig. 5. (b). Coefficient of drag vs flow-time when v = 5 m/s

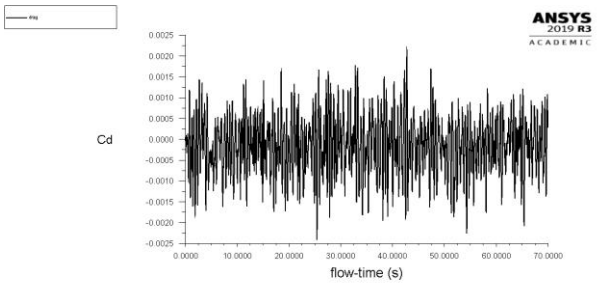

Fig. 5. (c). Coefficient of drag vs flow-time when v = 10 m/s

As the velocity increases the graph has more fluctuations. We consider the average value for the total flow-time and C_d in the third case is found to be highest. Hence we can say that C_d increases with increase in inlet velocity and hence the drag force too.

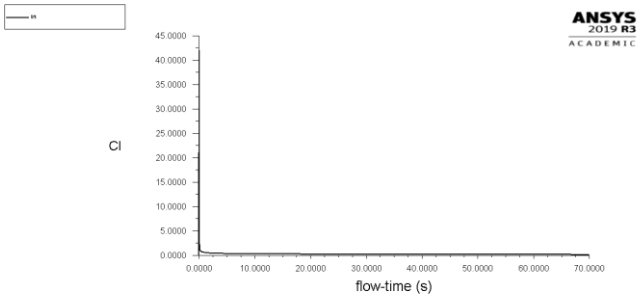

Fig. 6. (a). Coefficient of lift vs flow-time when v = 0.1 m/s

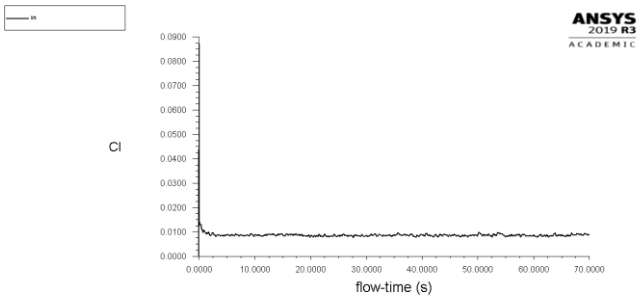

Fig. 6. (b). Coefficient of lift vs flow-time when v = 5 m/s

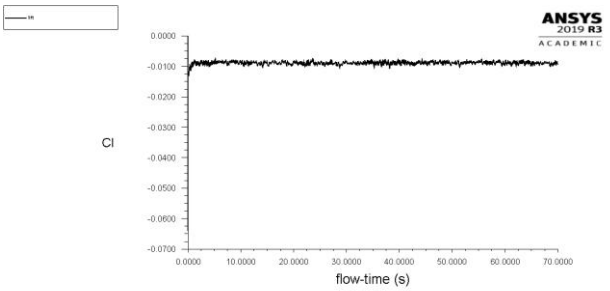

Fig. 6. (c). Coefficient of lift vs flow-time when v = 10 m/s

The coefficient of lift (C_l) is represented by Fig. 6. (a), Fig. 6. (b) and Fig. 6. (c) when the inlet velocity is 0.1 m/s, 5 m/s and 10 m/s respectively. When the inlet velocity is 0.1 m/s, the C_l value is almost zero which implies the lift force experienced by the semi-submersible is null. In Fig. 6. (b) the C_l value is 0.0100. In the third case, the velocity axis was reversed. Hence the negative value for C_l in Fig. 6. (c). But the graph is similar to that of the second case, but more number of fluctuations. Hence the difference between the average value of C_l of those two cases is pretty small. This tells us that the change in inlet velocity does not significantly affect the coefficient of lift or the lift force. For all the three simulations, we have used pressure-based solver. Absolute velocity formation is considered and the flow is transient. We have activated the Large Eddy Simulation (LES) turbulence model and the sub-grid scale model used is WALE. Coupled pressure-velocity scheme is selected. In spatial discretization, gradient is least squares cell based, pressure is of second order and momentum is bounded central differencing. Second order implicit transient formulation is chosen. Warped-face gradient correction is enabled. The flow courant number is 200. Explicit relaxation factors momentum and pressure are given value 0.75 each. Under relaxation factors density and body forces are equal to one. Standard initialization is done before the calculation in which the reference frame is relative to cell zone. The iteration is done for 7000 time-steps of size 0.01 each.

IV. CONCLUSION

The turbulent flow characteristics around a semi-submersible platform within a computational domain are numerically investigated. The turbulent flow is modelled by the computational fluid dynamics (CFD) approach using Large Eddy Simulation (LES) turbulence model. The stream line patterns, velocity contours and pressure contours are compared and analysed for different inlet velocities. It is identified that vortex shedding effect occurs at the centre of the semi-submersible and intensifies with the increase in inlet velocity. The columns, the pontoons and the bracings influence these motions. The coefficients of lift and drag experienced by the semi-submersible is plotted against the flow-time. We observed that though the magnitude of inlet velocity is influencing the coefficient of drag (C_d) considerably, it does not have much effect on coefficient of lift (C_l). The result from this study will be helpful in designing an effective semi-submersible platform and the ideal placing of it at proper locations for offshore applications.

REFERENCES

1. M. Liu, L. Xiao and L. Yang, Experimental investigation of flow characteristics around four square-cylinder arrays at subcritical Reynolds numbers, International Journal of Naval Architecture Ocean Engineering (2015), PP.7:906~919
2. R.T. Goncalves, G.F. Rosetti, A.L.C. Fujarra, A.C. Oliveira, Experimental study on vortex-induced motions of a semi-submersible platform with four square columns, Part I: Effects of current incidence angle and hull appendages, Ocean Engineering (2012), PP.150~169
3. J. Ma, D. Zhou, Z. Han, K. Zhang, Y. Bao, L. Dong, Fluctuating wind and wave simulations and its application structural analysis of a semi-submersible offshore platform, International Journal of Naval Architecture and Ocean Engineering (2019), PP.624~637
4. V. Holland, T. Tezdogan*, E. Oguz, Full-scale CFD investigations of helical strakes as a means of reducing the vortex induced forces on a semi-submersible, Ocean Engineering 137 (2017), PP.338~351
5. L. Xiao, M. Liu, Y. Liang, L. Tao, Experimental and numerical studies of the pontoon effect on vortex-induced motions of deep-draft semi-submersibles, Journal of Fluids and Structures 72 (2017), PP.59~79
6. H. Wei, L. Xiao, X. Tian, Y.M. Low, Nonlinear coupling and instability of heave, roll and pitch motions of semi-submersibles with bracings, Journal of Fluids and Structures 83 (2018), PP.171~193
7. X. Tian, H. Wei, L. Xiao, Ying Min Low, M. Liu, Effects of bracings and motion coupling on resonance features of semi-submersible platform under irregular wave conditions, Journal of Fluids and Structures 92 (2020), PP.102~783
8. R. Sharma, T.W. Kim, O.P. Sha and S.C. Misra, Issues in offshore platform research - Part 1: Semi-submersibles, International Journal of Naval Architecture and Ocean Engineering (2010), PP.2:155~170
9. A.C. Odijie, F. Wang, J. Ye, A review of floating submersible hull systems: Column stabilized unit, Ocean Engineering 144(2017), PP.191~202
10. H.R. Ghafari, M.J. Ketabdari, H. Ghassemi, E. Homayoun, Numerical study on the hydrodynamic interaction between two floating platforms in Caspian Sea environmental conditions, Ocean Engineering 188 (2019), PP.106~273

AUTHORS PROFILE

T Sai Shyam is a final year Btech Mechanical Engineering student at VIT University Chennai.

P R Jishnu is a final year Btech Mechanical Engineering student at VIT University Chennai.

Dr. R. Harish is working as an Assistant Professor in the school of Mechanical and Building Sciences at VIT Chennai campus. His research interests are in the field of computational fluid dynamics, Heat Transfer and Turbulent flows.